



Optics Letters

Efficient optical-to-terahertz conversion in large-area InGaAs photo-Dember emitters with increased indium content

I. E. ILYAKOV,^{1,2,*} B. V. SHISHKIN,¹ V. L. MALEVICH,^{3,4} D. S. PONOMAREV,⁵ R. R. GALIEV,⁵ A. YU. PAVLOV,⁵ A. E. YACHMENEV,⁵ S. P. KOVALEV,² M. CHEN,² R. A. AKHMEDZHANOV,¹ AND R. A. KHABIBULLIN^{5,6}

¹Federal Research Center Institute of Applied Physics of the Russian Academy of Sciences, Nizhny Novgorod 603950, Russia

²Helmholtz-Zentrum Dresden-Rossendorf, Bautzner Landstr. 400, 01328 Dresden, Germany

³Institute of Physics, National Academy of Sciences of Belarus, Minsk 220072, Belarus

⁴Belarus State University of Informatics and Radioelectronics, Minsk 220013, Belarus

⁵V.G. Mokerov Institute of Ultra High Frequency Semiconductor Electronics of the Russian Academy of Sciences, Moscow 117105, Russia

⁶Center for Photonics and Infrared Technology, Bauman Moscow State Technical University, Moscow 105005, Russia

*Corresponding author: igor_ilyakov@mail.ru

Received 21 April 2021; revised 11 June 2021; accepted 15 June 2021; posted 15 June 2021 (Doc. ID 428599); published 6 July 2021

In this Letter, optical-to-terahertz (THz) conversion of 800 nm femtosecond laser pulses in large-area bias-free InGaAs emitters based on photo-Dember (PD) and lateral photo-Dember (LPD) effects is experimentally investigated. We use metamorphic buffers to grow sub-micrometer thick $\text{In}_x\text{Ga}_{1-x}\text{As}$ layers with indium mole fractions $x = 0.37$, 0.53 , and 0.70 on a GaAs substrate. A strong enhancement of THz output energy with an increase of indium content is observed. On the surface of the sample providing the strongest emission ($x = 0.7$), we have fabricated a 1.5 cm^2 area of asymmetrically shaped metallic grating for LPD emission. This LPD emitter allows achieving high conversion efficiency of $0.24 \cdot 10^{-3}$ and a broad generation bandwidth of up to 6 THz. We also demonstrate that there is no significant difference in the conversion efficiency when operating at 1 and 200 kHz repetition rates. Our results show that large-area LPD emitters give a convenient, competitive way to generate intense high-repetition-rate THz pulses. © 2021 Optical Society of America

<https://doi.org/10.1364/OL.428599>

Laser-driven generation of terahertz (THz) waves (10^{11} – 10^{13} Hz) via downconversion of optical femtosecond pulses opens new horizons in spectroscopy and imaging [1]. The advantages of such an approach are an extremely broad bandwidth of the generated THz pulses and well-developed optical detecting methods routinely giving amplitude and phase characteristics of the generated signal. At the same time, this approach can be characterized by relatively low efficiency of optical-to-THz conversion, which limits the energy of the THz pulses. The high THz pulse energies can be achieved by using electro-optic crystals with record efficiencies reaching 10^{-4} – 10^{-2} levels depending on the pump laser wavelength and its energy [2–6]. However, this approach requires the usage

of the amplified laser systems with high optical fluences of 10 – 100 mJ/cm^2 , which also limits conversion efficiency at high repetition rates [5].

Unlike electro-optic crystals, photoconductor converters need much lower laser fluences. This type of optical-to-THz emitters consists of electrically biased and unbiased photoconductors. The first approach is based on transforming static electrical energy into the THz range using a laser pulse as a triggering switcher and needs additional biasing and antenna electrodes [7]. Using a multiple antenna array allows scaling up emitted THz power [8,9]. The alternative approach to biased photoconductive emitters is an optical-THz generation technique based on the photo-Dember (PD) effect [10]. This technique is free from the thermal noise originating from dark currents of electrically biased photoconductors and has the potential of reaching high conversion efficiencies at low laser fluence without external bias. To increase the PD emitter efficiency, a special metallic mask is used for generation of pulsed electrical currents parallel to the excited surface [11]. The so-called lateral photo-Dember (LPD) effect demonstrates a broad emission spectrum of up to 5 THz and allows scaling up the THz power by increasing the excitation area [11–14].

Despite the promising results demonstrated with PD and LPD THz emitters in the previous works, there is still a lack of information on the absolute value of conversion efficiency and its dependence on the material parameters. In fact, no value for the LPD emitter efficiency has been given in the literature up to date [10–14]. Besides, most studies of PD and LPD emitters are performed with tightly focused radiation of low-energy laser systems [10–15], which may limit the maximal conversion efficiency due to the small size of the emitting area compared with generated pulse wavelengths [16]. At the same time, growing demands for intense high-repetition-rate table-top sources of THz radiation stimulate research and development of optical-THz converters compatible with radiation of powerful

lasers [5,6]. Due to their rather low optical fluences, PD and LPD emitters with a scaled up emission area can be promising candidates for such converters.

In this Letter, we experimentally investigate THz emission from large-area InGaAs-based PD and LPD emitters with variable In content and propose their use for the generation of high-intensity high-repetition rate THz pulses. The samples are grown on GaAs substrates using metamorphic InAlAs buffers [17,18]. This growth procedure allows us to reach any desired concentration of In and consequently to vary the bandgap of InGaAs. Previously, the investigation of optimal bandgap of the PD emitters has been carried out only under the excitation by different wavelengths [12]. Here, we use samples grown by the same technology but with various In content (bandgap value) and study the conversion process particularly with a fixed excitation wavelength of 800 nm generated by the commonly used Ti:sapphire laser. Another benefit of the metamorphic buffer approach is the possibility of using the GaAs substrate, which is transparent to THz waves and allows convenient transmission geometry. In contrast to the previous works, where the LPD effect was observed in emitters with an area less than 1 mm^2 [10–14], we have developed a procedure of manufacturing large-area LPD emitters and conducted our studies on the 1.5 cm^2 area sample. The demonstrated conversion efficiency overcomes 10^{-4} level at 1 and 200 kHz repetition rates, and becomes comparable to record efficiencies reached with electro-optic crystals at high repetition rates [5,6].

Samples of $\text{In}_x\text{Ga}_{1-x}\text{As}$ photoconductors with indium mole fractions of $x = 0.37, 0.53,$ and 0.70 are grown by molecular-beam epitaxy on semi-insulating (100) GaAs substrates using a metamorphic growth technique [17,18]. A step-graded metamorphic buffer consisted of 5–7 $\text{In}_y\text{Al}_{1-y}\text{As}$ layers with the increase of the indium content by 10% in each consequent layer used for matching the lattice parameter between the GaAs substrate and the given composition of $\text{In}_x\text{Ga}_{1-x}\text{As}$. High crystalline quality of the grown samples is confirmed by means of high-resolution double-crystal X-ray diffraction. The surface of InGaAs samples has a typical metamorphic-growth cross-hatch morphology with RMS roughness of less than 15 nm measured by atomic force microscopy. To make an LPD emitter, a large-area metallic grating is formed on the surface of $\text{In}_{0.7}\text{Ga}_{0.3}\text{As}$. In order to generate a photo-induced current oriented parallel to the excited surface, the elements of metallic grating should have an asymmetric cross-sectional shape [12–14]. In particular, these elements have the form of wedges—with a sharp edge on one side and a rising slope of metal on the other. In Fig. 1, it can be seen that the $1.5 \mu\text{m}$ period grating is formed by 475 nm-high Ti/Al parallel bars which are fabricated using the electron-beam lithography and lift-off metallization. A thin $\sim 30 \text{ nm}$ gold layer is evaporated on the grating via inclined position of the sample to obtain a specific wedged shape because of the shadowing effect of the Al bars as it was demonstrated in [12]. The final Au-coated grating with a size of $10 \text{ mm}^2 \times 15 \text{ mm}^2$ has more than 6000 metal-semiconductor edges on the large-area LPD emitter surface. Here we use electron-beam lithography as a maskless technique for rapid prototyping of large-area grating. Technically, the described fabrication procedure gives the possibility to increase the grating area limited only by a substrate size and to vary the grating period.

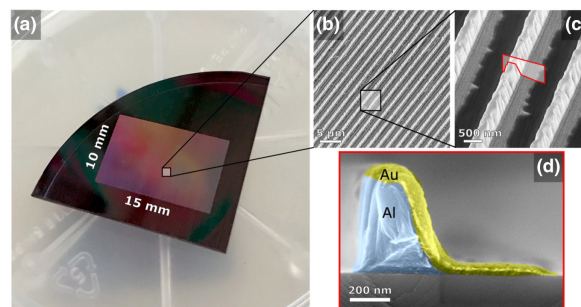


Fig. 1. $\text{In}_{0.7}\text{Ga}_{0.3}\text{As}$ with $10 \text{ mm}^2 \times 15 \text{ mm}^2$ large-area metallic grating. (a) Photo. (b), (c) Bird's eye-view SEM micrographs of the sample region with increasing magnification. (d) Cross section of the individual wedged bar [outlined red region from (c)].

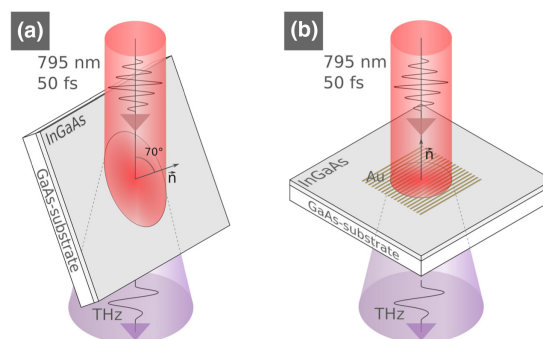


Fig. 2. Schematic diagram of the emission geometries: (a) femtosecond laser pulse is obliquely incident on the surface of InGaAs samples (PD generation scheme); (b) femtosecond laser pulse is normally incident on a surface of the $\text{In}_{0.7}\text{Ga}_{0.3}\text{As}$ sample with metal grating (LPD generation scheme).

The emission of THz pulses from the grown InGaAs samples is excited by Ti:sapphire laser pulses (up to 1 mJ, 50 fs, 795 nm, 1 kHz). The optical beam size is 7 mm at FWHM. The power and time-domain characteristics of the generated THz wave radiation are measured using a Golay cell and electro-optic sampling technique (with a 0.2 mm GaP crystal). The experiments are carried out under the two geometries of laser-THz excitation: (a) oblique laser pulse incidence for PD geometry [Fig. 2(a)]; and (b) normal laser pulse incidence for LPD geometry [Fig. 2(b)]. Typical waveforms and their Fourier-transform spectra of the generated THz pulses are presented in Fig. 3. All the samples in both PD and LPD geometries have the same spectral parameters: the maximum intensity occurs at around 1.5 THz, while a slow decay to a noise floor starts at 6 THz.

To investigate the PD generation [Fig. 2(a)] in semiconductors with different values of bandgap energy E_g , we measure THz emission from InGaAs samples with 0.37, 0.53, and 0.70 In content, which corresponds to $E_g = 0.916, 0.737,$ and 0.574 eV , respectively [19]. The lowest optical-to-THz conversion efficiency ($= 10^{-5}$) corresponds to the PD InGaAs-based emitter with 0.37 content of In and the highest ($= 0.8 \cdot 10^{-4}$) to the sample with the maximum In content of 0.7. The maximal efficiency for the samples in PD geometry is reached at a 70° incident angle. It corresponds to near-Brewster angle pumping and is approximately twice as high as the 45° laser incident angle often used in previous works. In addition, the samples are rotated around their normal, and no significant changes

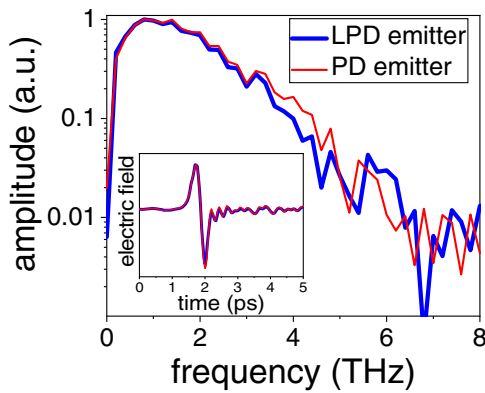


Fig. 3. Normalized typical time-domain and spectral dependences of THz pulses generated by PD and LPD emitters (0.7 In content).

in the THz emission are observed. The THz polarization is linear and orientated in the plane of incidence. Additionally, no signal is observed at normal laser incidence, which confirms that the main mechanism generating THz radiation in these samples is the PD effect, and additional influence of the second-order nonlinearity and thermal radiation is negligible. The radiation efficiency dependence on the fluence is shown in Fig. 4. The maximum efficiency for the samples is reached at the optical fluence of about $100 \mu\text{J}/\text{cm}^2$. With a further increase in the optical fluence, the optical-to-THz efficiency decreases, possibly due to the screening effect and saturation of optical absorption. Our results clearly demonstrate that the THz amplitude increases significantly with decreasing of E_g . This behavior can be explained by higher excess energy ($E_{\text{exc}} = h\nu - E_g$) and a higher gradient of the spatial distribution of photo-excited carriers (due to the higher optical absorption coefficient) in narrower bandgap semiconductors, which results in more efficient propagation of carriers towards the bulk [20]. The electron/hole mobility ratio is another important parameter affecting emission. However, the strong nonparabolicity of conduction band in a narrow bandgap InGaAs leads to an increase of the electron effective mass for high energy excitation levels. Theoretical modeling shows that under the impact of 800 nm laser pulses the high excess energy absorbed by charge carriers makes the contrast in mobilities nonsignificant when comparing GaAs, $\text{In}_{0.53}\text{Ga}_{0.47}\text{As}$, and InAs samples [20].

The LPD effect is investigated in the sample with the 70% In content, which demonstrates the highest efficiency in PD experiments. For the study in this Letter, the asymmetrically shaped metallic grating is fabricated on its surface as described above. Excitation with the laser pulses polarized along the metal wedges gives three times higher THz output power than with orthogonally polarized laser pulses. The polarization of the generated THz pulses is orthogonal to the stripes in both cases (along the thickness gradient of each wedge) as expected for the LPD effect. The maximum efficiency of the LPD emitter ($0.24 \cdot 10^{-3}$) is three times higher compared to the PD emitter. It is reached at normal incidence and much lower fluence ($2 \mu\text{J}/\text{cm}^2$) compared to the case of PD emission ($100 \mu\text{J}/\text{cm}^2$). The lower value of optimal fluence for the LPD emitter can be explained by additional laser field enhancement near the edges of the metallic grating deposited on the photoconductor surface. In agreement with [13], we also found that the excited electron current from which the THz emission originates is directed

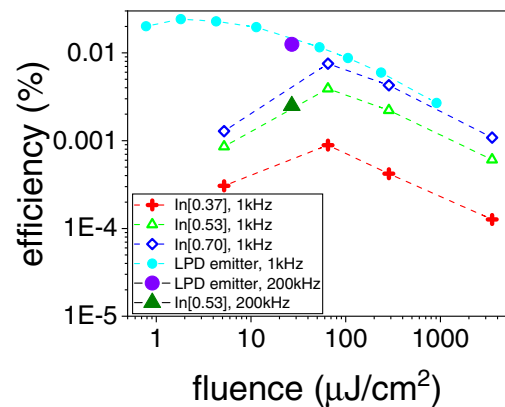


Fig. 4. Optical-to-THz efficiency at different laser fluences for 1 and 200 kHz (marked additionally on the graph) repetition rates. PD samples with In content: 0.37—red crosses, 0.53—green triangles (a dark green triangle for a 200 kHz repetition rate), and 0.70—blue rhombs. The LPD sample is denoted by cyan circles (violet circle for the 200 kHz repetition rate).

away from the thicker edge of the metal towards the unmasked region. This is determined by comparing the polarization of the emitted THz radiation from the LPD structure and from one of the PD samples (normal and oblique incidence, respectively). In the latter case, we assume that the electrons flow along the normal of the sample in the direction from surface to bulk.

The optical-to-THz conversion efficiency for the PD emitter with 0.53 In content and the LPD emitter (0.7 In content) are also measured with 200 kHz repetition rate excitation at optical fluence of $27 \mu\text{J}/\text{cm}^2$ (4.3 mm FWHM laser beam, $4 \mu\text{J}$ pulse energy, 800 nm, 100 fs). A pyroelectric detector placed after a 200 cm^{-1} low-pass filter, measures the THz power. For the LPD emitter, 800 mW of incident laser power has been converted to $100 \mu\text{W}$ THz output. In Fig. 4, similar values of conversion efficiencies for studied emitters at 200 and 1 kHz repetition rates are demonstrated.

Our results show that the efficiency strongly increases with the increase of In content due to the higher absorption coefficient and excess energy of the photo-excited carriers. One can expect a further increase of the efficiency by using the InAs layer, which can be fabricated within the same technological routine. Examination of other promising materials [14,15] for a large-area PD and LPD emitters may also lead to a further increase of conversion efficiency. The size, period, and shape of metallic grating can be optimized in terms of increasing efficiency as well [14]. Technically, the manufacturing procedure utilized in this Letter allows a widely varying period and width of the wedges.

The ability to reach high conversion efficiencies at low laser fluence is particularly beneficial for high-repetition-rate lasers, and the development of large-area emitters may be especially useful for producing high-repetition-rate and high-energy THz sources [5,6]. Such sources are currently based on large-scale accelerator machines and demonstrate their unprecedented capabilities in discovering new nonlinear effects in the THz range [21]. Although laser-based THz sources are currently less powerful, they are much more accessible and, due to their compactness, can be routinely integrated for pump-probe experiments in various facilities. Recently demonstrated record “laser-based” THz average powers of 144 and 66 mW for a lithium-niobate converter under 100 kHz, 3.44 mJ,

and 13.3 MHz, 17 μJ laser pulse impact give $0.42 \cdot 10^{-3}$ and $0.6 \cdot 10^{-3}$ conversion efficiencies [5,6], paving the way for linear and nonlinear high average power experiments. The maximal efficiency demonstrated here for the large-area LPD emitter is just 2-2.5 times smaller compared to the records in Refs. [5,6], and we do not observe any significant difference in the efficiency for 1 and 200 kHz repetition rates. At the same time, the generation bandwidth is significantly larger than in those experiments, which is of great demand when studying dynamic processes on fast sub-picosecond time scales. The large-area LPD emitter can be easily integrated into a high-power setup. For example, to convert a 1 mJ laser pulse to the THz range with 10^{-4} efficiency in the LPD emitter, one can use 100 $\mu\text{J}/\text{cm}^2$ fluence and a sample with a 3.6 cm diameter, which can be fabricated by the approach presented here. Due to rather low fluence needed for efficient conversion, we also expect LPD emitters to efficiently operate far beyond the 200 kHz repetition rate demonstrated here.

In conclusion, we study optical-to-THz conversion of Ti:sapphire laser radiation in large-area InGaAs photoconductors with different In contents grown on GaAs substrate. In particular, optical-to-THz conversion originating from PD emitters demonstrates up to an order increase in efficiency when the In content in $\text{In}_x\text{Ga}_{1-x}\text{As}$ increases from $x = 0.38$ to $x = 0.7$. The highest efficiency of $0.8 \cdot 10^{-4}$ ($x = 0.7$) is achieved at optical fluence of 100 $\mu\text{J}/\text{cm}^2$. The generated spectra continuously cover the frequency range up to 6 THz. Making a large-area (over 1 cm^2) metallic grating on the sample with the highest In content ($x = 0.7$) leads to a further efficiency increase due to the LPD effect (up to $0.24 \cdot 10^{-3}$; achievable even at much lower fluence of 2 $\mu\text{J}/\text{cm}^2$). To the best of our knowledge, the absolute conversion efficiency for LPD emitters is being reported for the first time. The demonstrated molecular-beam epitaxy growth procedure allows reaching any desired concentration of In and allows making structures for LPD emission with large areas limited only by the substrate size. The conversion efficiency of PD and LPD emitters remains high as the repetition rate of femtosecond laser is increased from 1 to 200 kHz. The demonstrated conversion efficiency is comparable to ones very recently reached at high repetition rates using electro-optic crystals [5,6], while the generation bandwidth in our case is significantly larger.

Our results show that the combination of low optical laser fluences with a scaled up emission area makes LPD emitters an effective competitive way of generating intense high-repetition-rate THz pulses demanded for numerous experimental investigations. We believe that careful examination of other photoconductive materials and optimization of the metallic grating parameters for large-area emitters might lead to further progress in this direction.

Funding. Institute of Applied Physics, Russian Academy of Sciences (0030-2021-0004); Russian Science Foundation (19-79-10240).

Disclosures. The authors declare no conflicts of interest.

Data Availability. Data underlying the results presented in this paper are not publicly available at this time but may be obtained from the authors upon reasonable request.

REFERENCES

1. P. U. Jepsen, D. G. Cooke, and M. Koch, *Laser Photonics Rev.* **5**, 124 (2011).
2. S. B. Bodrov, I. E. Ilyakov, B. V. Shishkin, and A. N. Stepanov, *Appl. Phys. Lett.* **100**, 201114 (2012).
3. S. B. Bodrov, I. E. Ilyakov, B. V. Shishkin, and M. I. Bakunov, *Opt. Express* **27**, 36059 (2019).
4. X. Wu, S. Carbajo, K. Ravi, F. Ahr, G. Cirmi, Y. Zhou, O. D. Mücke, and F. X. Kärtner, *Opt. Lett.* **39**, 5403 (2014).
5. P. L. Kramer, M. K. R. Windeler, K. Mecseki, E. G. Champenois, M. C. Hoffmann, and F. Tavella, *Opt. Express* **28**, 16951 (2020).
6. F. Meyer, T. Vogel, S. Ahmed, and C. J. Saraceno, *Opt. Lett.* **45**, 2494 (2020).
7. A. E. Yachmenev, D. V. Lavrukhin, I. A. Glinskiy, N. V. Zenchenko, Y. G. Goncharov, I. E. Spektor, R. A. Khabibullin, T. Otsuji, and D. S. Ponomarev, *Opt. Eng.* **59**, 061608 (2020).
8. M. Awad, M. Nagel, and H. Kurz, *Appl. Phys. Lett.* **91**, 181124 (2007).
9. M. Beck, H. Schäfer, G. Klatt, J. Demsar, S. Winnerl, M. Helm, and T. Dekorsy, *Opt. Express* **18**, 9251 (2010).
10. V. Apostolopoulos and M. E. Barnes, *J. Phys. D: Appl. Phys.* **47**, 374002 (2014).
11. G. Klatt, F. Hülser, W. Qiao, M. Beck, R. Gebbs, A. Bartels, K. Huska, U. Lemmer, G. Bastian, M. B. Johnston, M. Fischer, J. Faist, and T. Dekorsy, *Opt. Express* **18**, 4939 (2010).
12. G. Klatt, B. Surrer, D. Stephan, O. Schubert, M. Fischer, J. Faist, A. Leitenstorfer, R. Huber, and T. Dekorsy, *Appl. Phys. Lett.* **98**, 021114 (2011).
13. M. E. Barnes, S. A. Berry, P. Gow, D. McBryde, G. J. Daniell, H. E. Beere, D. A. Ritchie, and V. Apostolopoulos, *Opt. Express* **21**, 16263 (2013).
14. J. Wallauer, C. Grumber, V. Polyakov, R. Iannucci, V. Cimalla, O. Ambacher, and M. Walthers, *Appl. Phys. Lett.* **107**, 111102 (2015).
15. I. Nevinkas, K. Vizbaras, A. Trinkunas, R. Butkute, and A. Krotkus, *Opt. Lett.* **42**, 2615 (2017).
16. J. Z. Xu and X.-C. Zhang, *Opt. Lett.* **27**, 1067 (2002).
17. D. S. Ponomarev, A. Gorodetsky, A. E. Yachmenev, S. S. Pushkarev, R. A. Khabibullin, M. M. Grekhov, K. I. Zaytsev, D. I. Khuyainov, A. M. Buryakov, and E. D. Mishina, *J. Appl. Phys.* **125**, 151605 (2019).
18. D. S. Ponomarev, R. A. Khabibullin, A. E. Yachmenev, P. P. Maltsev, M. M. Grekhov, I. E. Ilyakov, B. V. Shishkin, and R. A. Akhmedzhanov, *Semiconductors* **51**, 509 (2017).
19. S. Adachi, *Physical Properties of III-V Semiconductor Compounds* (Wiley, 1992).
20. M. Alfaro-Gomez and E. Castro-Camus, *Appl. Phys. Lett.* **110**, 042101 (2017).
21. H. A. Hafez, S. Kovalev, J.-C. Deinert, Z. Mics, B. Green, N. Awari, M. Chen, S. Germanskiy, U. Lehnert, J. Teichert, Z. Wang, K.-J. Tielrooij, Z. Liu, Z. Chen, A. Narita, K. Müllen, M. Bonn, M. Gensch, and D. Turchinovich, *Nature* **561**, 507 (2018).